applied sciences

MDPI

Article

Bioimaging Using Full Field and Contact EUV and SXR Microscopes with Nanometer Spatial Resolution

Przemysław Wachulak [1,*], Alfio Torrisi [1], Mesfin Ayele [1], Joanna Czwartos [1], Andrzej Bartnik [1], Łukasz Węgrzyński [1], Tomasz Fok [1], Tomáš Parkman [2], Šárka Salačová [2], Jana Turňová [2], Michal Odstrčil [3] and Henryk Fiedorowicz [1]

1 Institute of Optoelectronics, Military University of Technology, 2 Kaliskiego Street, 00-908 Warsaw, Poland; atorrisi83@gmail.com (A.T.); mgetachew11@gmail.com (M.A.); jczwartos@wat.edu.pl (J.C.); abartnik@wat.edu.pl (A.B.); lwegrzynski@wat.edu.pl (L.W.); tfok@wat.edu.pl (T.F.); hfiedorowicz@wat.edu.pl (H.F.)

2 Faculty of Biomedical Engineering, Czech Technical University in Prague, 272 01 Kladno, Czech Republic; tomasparkman@gmail.com (T.P.); sarka.salacova@fjfi.cvut.cz (S.S.); turnojana@gmail.com (J.T.)

3 Paul Scherrer Institut, CH-5232 Villigen PSI, Switzerland; michal.odstrcil@psi.ch

* Correspondence: przemyslaw.wachulak@wat.edu.pl; Tel.: +48-261-839-540

Academic Editor: Dermot Brabazon
Received: 18 April 2017; Accepted: 23 May 2017; Published: 26 May 2017

Abstract: We present our recent results, related to nanoscale imaging in the extreme ultraviolet (EUV) and soft X-ray (SXR) spectral ranges and demonstrate three novel imaging systems recently developed for the purpose of obtaining high spatial resolution images of nanoscale objects with the EUV and SXR radiations. All the systems are based on laser-plasma EUV and SXR sources, employing a double stream gas puff target. The EUV and SXR full field microscopes—operating at 13.8 nm and 2.88 nm wavelengths, respectively—are currently capable of imaging nanostructures with a sub-50 nm spatial resolution with relatively short (seconds) exposure times. The third system is a SXR contact microscope, operating in the "water-window" spectral range (2.3–4.4 nm wavelength), to produce an imprint of the internal structure of the investigated object in a thin surface layer of SXR light sensitive poly(methyl methacrylate) photoresist. The development of such compact imaging systems is essential to the new research related to biological science, material science, and nanotechnology applications in the near future. Applications of all the microscopes for studies of biological samples including carcinoma cells, diatoms, and neurons are presented. Details about the sources, the microscopes, as well as the imaging results for various objects will be shown and discussed.

Keywords: gas puff target; Fresnel zone plates; EUV/SXR microscopy; contact microscopy; imaging; nanometer resolution

1. Introduction and Previous Achievements

Advancements in nanoscience and nanotechnology require tools and methods for nanometer scale resolution imaging. Affecting the matter on nanoscale and subsequent observation of those manipulations is a key factor in the rapid development of nanotechnology. Among the methods employing visible light radiation [1,2] to image matter at nanometer scales shorter wavelengths are also used, for example in extreme ultraviolet (EUV) and soft X-ray (SXR) microscopy experiments [3]. EUV and SXR microscopy has been proven as useful tools for imaging of objects with nanometer spatial resolution, having advantages such as obtaining additional information about the objects investigated, providing at the same time high optical contrast in the specific wavelength ranges used for this purpose. The main characteristics of the EUV radiation are its strong absorption in very thin layers of materials, so it provides a good optical contrast in thin films and layers of materials. On the

other hand, SXR radiation—specifically in the so-called "water-window" (λ = 2.3–4.4 nm)—proved to be particularly useful for high resolution imaging of biological samples, because of high optical contrast existing between carbon and water present in those samples.

Imaging in short wavelength ranges requires a high photon flux. It is the main reason why, until the development of compact sources, most of the studies in the field of EUV and SXR microscopy were conducted using synchrotron and free-electron laser facilities [4–6]. Such facilities are still being used not only for the purpose of high resolution imaging, but also for cutting-edge scientific experiments, providing the highest available photon flux, with the possibility to tune the generated wavelength and producing beams with adjustable spatial and temporal coherence. Nevertheless, these sources present some drawbacks because of their high complexity, high maintenance costs, requirement for highly trained staff present during the experiments and, finally, limited user access. Thus, to mitigate those difficulties, the recent progress in development of a new generation of compact EUV and SXR compact sources was made over the last few decades. Nowadays, there are sources which can perform certain experiments, previously restricted to large scale facilities, on a much larger scale in smaller laboratories worldwide. These experiments include imaging with nanometer spatial resolution.

Laser-produced plasma sources, emitting short wavelength radiation in the SXR and EUV spectral ranges, offer an important alternative to be the drivers dedicated for compact imaging systems [7,8]. They can overpass the limited accessibility of large facilities, maintaining a comparable spatial resolution [9,10]. Over the last few years, many efforts have been made to perform nanometer spatial resolution imaging in the EUV and SXR spectral ranges employing both large scale and compact sources. The synchrotron radiation at λ = 2.4 nm was used for imaging frozen-hydrated samples at atmospheric pressure [11] to observe internal details of algae with a spatial resolution of ~35 nm. Using the Advanced Light source synchrotron facility, a 10 nm spatial resolution imaging was obtained at 1.75 nm wavelength both in full-field and in scanning mode [12]. Recently, a novel approach was demonstrated, so-called dark-field X-ray microscopy, which is a non-destructive microscopy technique for the three-dimensional mapping of orientations and stresses [13]. Such a technique allowed multiscale imaging with a spatial resolution of ~100 nm. The various capabilities of full-field transmission X-ray microscopy, 3D X-ray tomography, Zernike phase contrast, quantification of absorption, and chemical identification via X-ray fluorescence and X-ray absorption near edge structure imaging is now also possible with synchrotron light [14] for characterization of biomaterials.

The compact sources are also being widely used for the purpose of high spatial resolution imaging in the EUV/SXR range. An SXR source, emitting at λ = 2.88 nm, based on a liquid jet nitrogen target, was employed recently for microscopy in the 'water-window' range with a sub-50 nm spatial resolution, but this system presents very complicated hardware [15]. Another nano-imaging technique is represented by the employment of compact high order harmonic generation (HHG) sources for sub-100 nm spatial resolution [16,17]. The HHG systems, however, require a femtosecond laser as a driver for HHG process. Also, typical HHG conversion efficiency (~10^{-6}–10^{-4}) often results in long exposures or does not allow a proper reconstruction of the image. Ptychographic techniques usually based on employment of hard X-ray beams are also possible, providing a very high spatial resolution, but they are extensively time consuming [18]. Imaging in the EUV range can be used to analyze very thin samples, nanofilms, and nanostructures. That is because the EUV radiation is absorbed by solid materials with thicknesses of the order of ~100 nm [19] and by gaseous materials with thicknesses of the order of a few millimetres [20]. It was demonstrated that the radiation from a capillary discharge laser operating at a wavelength of λ = 46.9 nm EUV can obtain images with a spatial resolution better than 55 nm [21,22], and that the spatial resolution of holographic images employing the same wavelength, can be improved up to sub-50 nm [23]. A solid-state target based table top EUV laser, emitting 13.2 nm wavelength radiation from Ni-like Cd ions, was employed for imaging with a sub-38 nm spatial resolution [24]. Using a xenon gas discharge source, a sub-100 nm zone-plate based EUV microscope with zooming was demonstrated. This system combines Schwarzschild objective and a zone plate for second stage magnification [25]. Very nice results were also recently demonstrated by

Legall et al. [26], using a liquid nitrogen target based system and a 1.3 kHz repetition rate Nd:YAG laser to record images of biological samples and nanostructures with half-pitch spatial resolution of 40–50 nm. The only drawbacks are that it is a quite complicated system and it is larger than other sources. Another interesting and already well established technique for obtaining high resolution images of samples is a projection imaging called contact microscopy. This method uses EUV and SXR radiation transmitted through the sample to expose a high-resolution photoresist underneath, being in contact with the sample. Using this method, first imprints of human blood platelets [27], fibroblasts [28], diatoms [29], and hydrated biological cells [30] were obtained.

Since there is no ideal solution for the source at the moment, it is necessary to find a good compromise in desktop SXR/EUV imaging systems, between the performance—namely, high photon flux; possibility to obtain high spatial resolution images with low exposure time; and the complexity, size, cost of these setups, which is still the main limitation of short wavelength photon-based microscopes disallowing their wide-spread. Some of these problems can be addressed employing double stream gas puff target laser plasma sources for microscopy purposes. Such a source, which has been developed initially for EUV metrology applications in the frame of MEDEA+ project [31], was also recently used for surface modification of polymers for biocompatibility improvement [32] or for radiobiology applications [33]. The double stream gas puff target sources, coupled with zone plates (FZPs) optics or as illumination sources for contact microscopy, represent a very useful technique for lab-scale analysis in order to perform high spatial resolution imaging by using short wavelength radiations.

Thus, in this article, we would like to present our recent activities related to the development and possible applications of three simple and compact SXR/EUV microscopes, capable of resolving 50–80 nm features. Those systems require short exposure times and have a desktop footprint. The source employed can generate the plasma efficiently, without debris production. The microscopes are easy to operate and have compact construction. Moreover, the EUV/SXR microscopes, based on those sources [34], do not require sample preparation such as gold coating for SEM microscopes or staining and marking like in STED. In such systems, the gas puff target is produced by the injection of a small amount of high-Z gas—working gas, into a stream of low-Z gas—outer gas, by a fast electromagnetic double valve system, as depicted in Figure 1a. The gas puff target is then irradiated by focused laser pulses from a Nd:YAG laser. The interaction of a laser pulses with gaseous target allows generation of the EUV and SXR radiation. Both full-field microscopes use reflective optics to focus the short wavelength radiation onto a sample and FZPs to obtain magnified images of the sample with high spatial resolution. The contact microscope uses the spectrally filtered plasma radiation directly, without pre-focusing, to form an imprint of the sample in the photoresist layer.

These microscopes may represent an important alternative to performing experiments in small academic laboratories on a much larger scale than with the employment of synchrotron facilities and could have a significant effect on the nanotechnology development in the near future. The goal of developing these microscopes is to show feasibility to achieve high resolution imaging, low exposure times, together with a compact footprint, which may in the future open a possibility for commercialization.

2. Materials and Methods

2.1. The EUV and SXR Microscopes

Soft X-ray contact microscope and the full-field EUV/SXR microscopes are schematically depicted in Figure 1b–d, respectively. The sources for those microscopes are based on a compact Nd:YAG laser, λ = 1064 nm, 0.5–0.7 J pulse energy, 3 ns pulse duration, and 1–10 Hz repetition rate. The laser beam is focused onto a double-stream gas puff target, which is schematically depicted in Figure 1a.

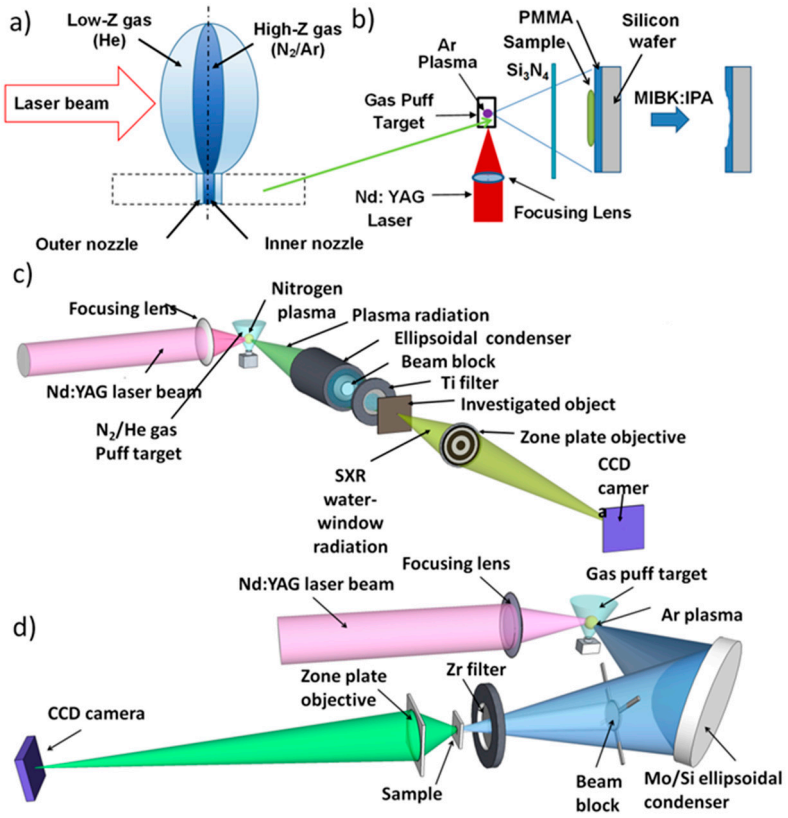

Figure 1. (**a**) Scheme of the double stream gas puff target employed in laser-plasma EUV/SXR sources, (**b**) scheme of the contact SXR microscope, (**c**) scheme of the SXR full-field microscope, and (**d**) scheme of the EUV full-field microscope employing off-axis condenser geometry.

The target is produced by an electromagnetic valve with double radially-symmetric nozzles. Laser pulses irradiate the gaseous target producing plasma. The plasma emits radiation in various spectral ranges, including the EUV and SXR regions of electromagnetic spectrum. Depending on the spectral range and on the type of the microscope, the gas puff target source was optimized for efficient emission in the "water window" (both quasi-monochromatic for the SXR full-field microscope and broadband for contact SXR microscope) and the EUV spectral range, using spectral narrowing with thin metal filters. A nitrogen plasma radiation, filtered with a Ti foil, provides λ = 2.88 nm wavelength radiation and an Ar plasma emission, filtered with Mo/Si multilayer mirror and Zr filter provides radiation at λ = 13.84 nm. However, for the argon plasma, if a silicon nitride filter is used, it provides emission from 2.8 to 4 nm with much larger number of photons than in case of nitrogen plasma, suitable for contact microscopy. Such sources were employed for SXR and EUV experiments, respectively. The gas pressures, nozzle position in respect to the laser focus, and valve timing in respect to the laser pulse were optimized in order to maximize the photon flux at the sample plane. The inner nozzle injects a small amount of working gas (high Z gas—N_2 at 8 bar, in case of SXR full-field microscope, and Ar, at 10 bar, in case of the EUV full-field microscope and contact SXR microscope), while the outer nozzle injects an outer gas (low Z gas—He, with a pressure of 6 bar), to narrow down the flow of the working gas, reducing its density gradient along the nozzle axis. Such an approach can obtain higher target density by confining the target gas flow and, in turn, allows for higher photon yield in the EUV/SXR region. Such radiation is then focused using condenser optics and illuminates the sample, Figure 1c,d, located in a second focal point of a condenser in the case of full-field microscopes. Depending on the type of microscope, plasma radiation is collected and focused by a different condenser and filter, and images of the objects are obtained with different zone plates using a back-illuminated charge-coupled device (CCD) camera. In the case of contact SXR microscope the scheme is much simpler, as can be

seen in Figure 1b, because radiation from the plasma is transmitted through a 200 nm thick Si_3N_4 filter and illuminates the sample directly to form its imprint in the surface of the photoresist. In the following paragraphs, the systems will be described in more detail.

2.2. SXR Full-Field Microscope

To focus the SXR radiation from the nitrogen plasma an ellipsoidal, axi-symmetrical SXR condenser (Rigaku, Prague, Czech Republic) coated with nickel film was used, as depicted in Figure 1c. A titanium filter (200 nm thick, Lebow Co., Goleta, CA, USA), positioned downstream the condenser, selects the He-like nitrogen line at λ = 2.88 nm from nitrogen plasma emission, suitable for the objective optic. Filtered SXR radiation illuminates the sample/object, positioned 140 mm downstream the condenser, in the second focal point. A FZP objective (Zoneplates Ltd., Claverings Industrial Estate, London, UK) was used to form a magnified image onto a back-illuminated SXR-sensitive CCD camera (Andor, iKon-M DO-934-BN, 1 Mpixel, 13 $\times$ 13 μm^2 pixel size) in transmission mode. A silicon nitride FZP (400 nm thick, 250 µm in diameter, outer zone width of 30 nm) with a focal length f = 2.6 mm at 2.88 nm wavelength, was used as an objective. The numerical aperture of the zone plate was matched to the numerical aperture of the condenser, providing incoherent illumination [35]. The image plane was located 57 cm from the zone plate resulting in the geometrical magnification of the system of ~220×. It was already demonstrated that such a system is capable to achieve a half-pitch spatial resolution of ~60 nm [36] (corresponding to half-period of the grating imaged under incoherent illumination conditions for a given numerical aperture of the objective—smallest feature that the microscope can resolve). More details about the microscope and its technical component can be found in [37]. The photograph of this system is depicted in Figure 2a.

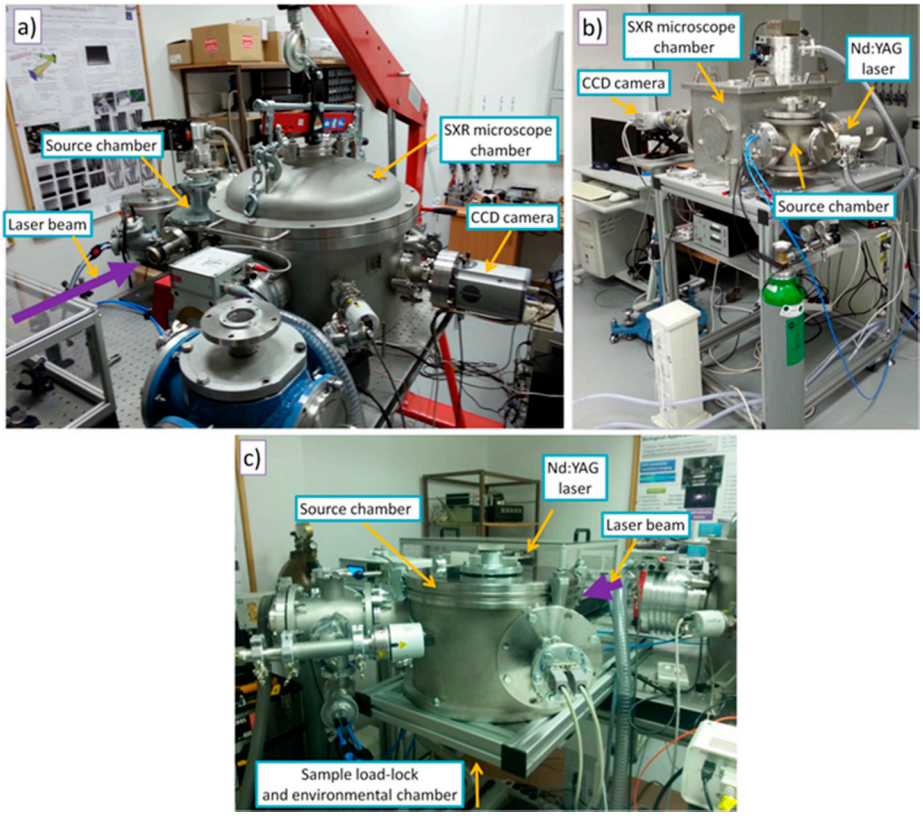

Figure 2. Photographs of three EUV/SXR imaging systems: (**a**) photograph of the SXR full-field microscope, (**b**) photograph of the EUV full-field microscope, and (**c**) photograph of the contact SXR microscope developed at the Institute of Optoelectronics, Military University of Technology, Warsaw.

2.3. EUV Full-Field Microscope

In this system, Ar plasma radiation was collected and spectrally filtered using an ellipsoidal off-axis mirror coated with Mo/Si multilayers. This mirror was employed as a condenser (Reflex S.R.O., Prague, Czech Republic—substrate and IOF, Jena, Germany—coating). The condenser was designed and manufactured in order to reflect the radiation at the wavelength of 13.5 $\pm$ 0.5 nm at 45° incidence angle in off-axis geometry. To eliminate longer wavelengths emitted from the Ar plasma (at wavelengths $\lambda > 16$ nm) a 250 nm thick zirconium filter (Lebow Co., Goleta, CA, USA) was used. The sample was imaged using a Fresnel Zone Plate (FZP) objective (diameter 200 µm, number of zones 1000 and outer zone width $\Delta r = 50$ nm, made in 200 nm thick PMMA on top of a 50 nm thick Si_3N_4 membrane (Zoneplates Ltd., Claverings Industrial Estate, London, UK) onto the CCD camera (Andor, iKon-M DO-934-BN camera, Andor Technology Ltd., Belfast, UK). As in the case of the SXR microscope, an incoherent illumination was provided by matching the numerical aperture of the condenser and of the FZP objective. The geometrical magnification of the objective was 410×, however, it can be easily changed by adjusting the FZP-CCD distance. Such a system, in this configuration, is capable to achieve a half-pitch spatial resolution of 48 nm [38]. More details about this system can be found in [39]. The photograph of this system is depicted in Figure 2b.

2.4. SXR Contact Microscope

In the third system, the Ar plasma emission was tailored to the "water-window" spectral range by employing 200 nm thick Si_3N_4 window. In this case, the monochromaticity of the radiation is not necessary, contrary to the previous cases, in which Fresnel zone plates were employed. Using a silicon nitride filter, most energy will reside in the wavelength range from 2.8 nm to 4 nm, well within the "water window" range. The higher energy photons, $\lambda < 2$ nm wavelength, are not produced, because limited energy of the laser pulses and their time durations cause plasma to be insufficiently hot to emit efficiently at higher energies, while the lower energy photons will be blocked by decaying edge of the transmission curve of silicon nitride filter. Such broad-band SXR radiation from Ar/He gas puff target has approximately one order of magnitude more photons compared to N_2/He gas puff target, which in this case allows for the irradiation and exposure of the high resolution photoresist (500 nm thick PMMA on top of a silicon wafer) acting as a detector. The object investigated is then placed in contact with the PMMA. The light that is locally transmitted by the object's structure illuminates the photoresist and changes its physical and chemical structure. After irradiation, the photoresist is chemically developed in a solution of methyl isobutyl ketone and isopropyl alcohol (MIBK:IPA 1:2 v/v) for 90 s to 3 min (depending on the experiment) and modulation of the light intensity absorbed by the object is converted in this process to a modulation of the thickness of the resist. This creates a relief-like structure in its surface. The height of the relief structure is directly proportional to the dose of radiation absorbed in the resist volume. In such a process, a high-resolution imprint of the internal structure of the object can be stored in the near-surface of the photoresist and later converted to an image using AFM or SEM microscopes. More details about this system can be found in [40]. The photograph of this system is depicted in Figure 2c.

3. Imaging with Compact EUV and SXR Microscopes Based on a Laser Plasma Sources

All experimental systems mentioned in this paper were developed at the Institute of Optoelectronics, Military University of Technology, Warsaw, Poland. Those systems were also extensively used to image test samples for resolution assessment, and the real samples—such as nanostructures, biological samples, organic, and inorganic samples, among others. A few examples of such experiments will be presented in this section.

3.1. SXR Full-Field Imaging

Two examples of "water window" images of organic samples, acquired with the full-field SXR microscope are depicted in Figure 3. Figure 3a,b show a sample of CT-26 fibroblast from Mus musculus colon carcinoma (strain BALB/c), prepared on top of a 30 nm thick Si_3N_4 membrane. A direct comparison between the image acquired with a traditional optical microscope (Figure 3a) and the SXR microscope image (Figure 3b), acquired with 200 SXR pulses, at a source repetition rate of 10 Hz, exposure time of 22 s, and detector (CCD) temperature of −20 °C, are shown. The sample was prepared with a gradual dehydration in ethanol series (final concentration 70% EtOH), without any fixation procedure. The SXR image shows improved spatial resolution due to the employment of a shorter wavelength, beyond the diffraction limit of the optical-visible light microscopes. Some internal and external structures can be distinguished due to phase contrast in the visible light microscopy images and due to the modulation in the absorption of the SXR light through the sample in the SXR images.

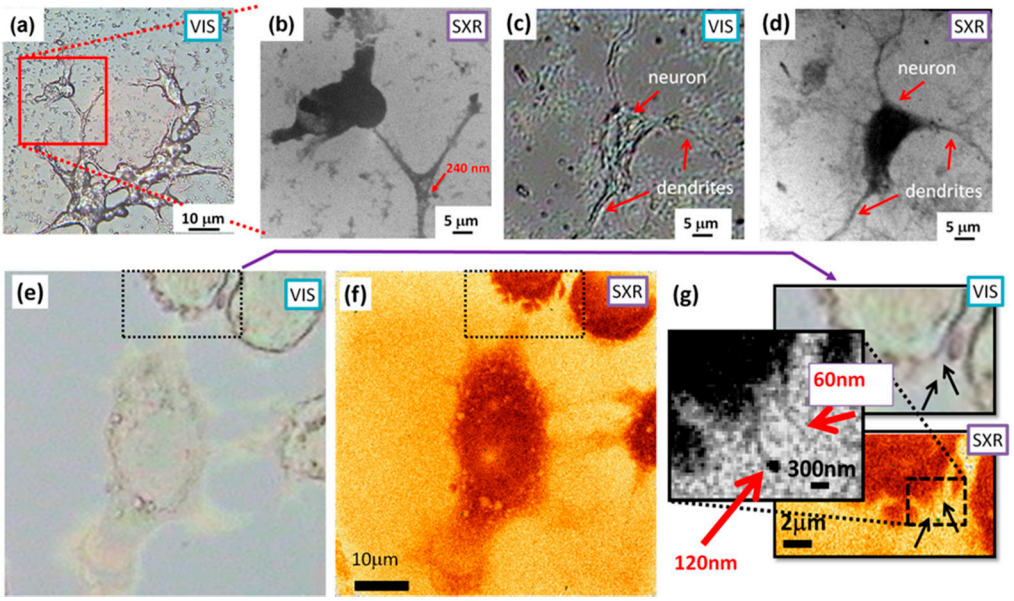

Figure 3. CT 26 fibroblast cells. Comparison of the optical image (**a**) and detail image (**b**) with the SXR "water window" microscope (red square in (**a**)) that shows small features of the order of 240 nm (indicated with a red arrow). (**c**) and (**d**) show a comparison of the mouse hippocampal neuron, acquired with optical microscope (40× objective, mag. 400×) and SXR microscope, respectively, showing a single neuron with dendrites branching out. (**e**) and (**f**) show colon carcinoma cells images with visible light microscope and the SXR microscope, respectively, while (**g**) depicts some smallest features visible in those images, indicating features comparable to the spatial resolution of the SXR microscope.

Figure 3e,f show improvements in the spatial resolution. The carcinoma cells (visible light microscope—VIS, and the SXR microscope—SXR labels) with insets depicting zoomed regions indicated with dotted boxes—Figure 3g. Some external structures of the cells cannot be recognized in visible light microscope images, while they are visible in the SXR microscope with features being ~60 nm in size, approaching the spatial resolution of the microscope.

A second example consists on hippocampal neurons from E17 mouse embryos, cultured for 10 days on poly-D-lysine coated, 50 nm thick Si_3N_4 substrates before fixation in 4% PFA in 20% sucrose PBS, followed by dehydration from 100 to 70% ethanol and air drying. The neurons were also imaged using both microscopes: visible light microscope (40× objective, 400× magnification)—Figure 3c, and the SXR microscope (sample to CCD magnification of 410×, exposure of 200 SXR pulses, 20 s)—Figure 3d. The comparison with the optical image (Figure 3c) shows a significant improvement of the spatial resolution employing the "water window" radiation. In this case, it is possible to observe

that the high absorption coefficient at SXR wavelengths enhances the optical contrast to the point that a barely visible neuron in Figure 2c is much better visualized in Figure 2d. In the SXR image, it is possible to distinguish the neuron and dendrites that are blurred due to inferior resolution and phase-type imaging using the optical microscope.

Except for the CCD background removal, adjustment of their brightness, and increased contrast in the inset of Figure 3g to show the smallest observable features, the SXR images were not altered in any other way.

3.2. EUV Full-Field Imaging

In this experiment CT26 fibroblast cells, Chrysodidimus cells and diatoms were imagined using the EUV microscope and visible light microscope. The EUV images were acquired with 200 EUV pulses—22 s exposure time and detector temperature of −20 °C. A sample of CT 26 cells fixed with 30% hexamethildisilazane (HDMS) in absolute EtOH on top of 30 nm Si_3N_4 membrane was imaged with the visible light microscope (VIS) as depicted in Figure 4a and at 13.84 nm wavelength with the EUV microscope—Figure 4b. It can be seen that the EUV image shows a very high contrast and resolution enhancement and permits to investigate features of the order of 100 nm or smaller in size.

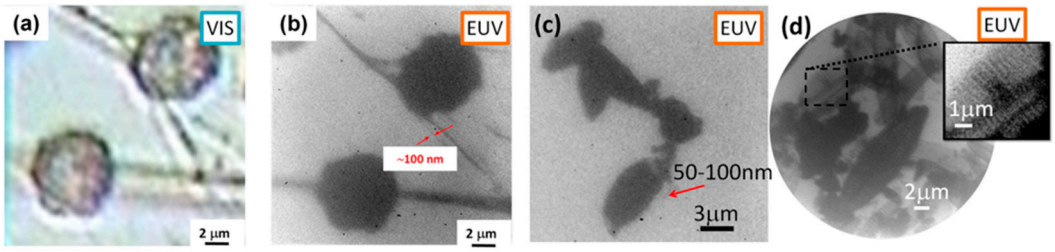

Figure 4. Comparison of CT 26 fibroblast cells sample acquired with optical microscope (**a**) and the EUV microscope (**b**). It is possible to recognize small features of the order of 100 nm (as indicated in red arrows) in the EUV image. The EUV image of Chrysodidimus cells (**c**) and diatoms (**d**) obtained with exposure of 100–200 EUV pulses. Features as small as 50–100 nm are visible.

Chrysodidimus cells imaged using the EUV microscopes can be seen in Figure 4c, while the diatoms deposited on top of 30 nm thick Si3N_4 membrane are depicted in Figure 4d, with a small inset showing diatom structures as small as a few hundred of nanometers. The EUV images exhibit superior spatial resolution and much higher optical magnification (410×) comparing to visible light microscopy—Figure 4a.

Except for the CCD background removal, adjustment of their brightness and increased contrast in the inset of Figure 4d to show the smallest observable features, the EUV images were not altered in any other way.

3.3. SXR Contact Microscopy Imaging

The contact microscope has been used for imaging of T24 (transitional cancer cell of the urine bladder, ATCC), which was prepared in collaboration with the Institute of Nuclear Physics Krakow, Poland. The cells were grown in culture flasks (Sarstedt AG & Co., Nümbrecht, Germany) in a RPMI 1640 medium (Sigma-Aldrich Sp. z.o.o, Poznan, Poland) supplemented with 10% foetal calf serum (Sigma, pH 7.4) and with 1% mixture of antibiotics (streptomycin, neomycin, and penicillin, Sigma-Aldrich Sp. z.o.o, Poznan, Poland), at 37 °C in 95%air/5%CO_2 atmosphere. After a few passages, the cells were trypsinized using 0.05% in EDTA-trypsin solution (Sigma-Aldrich Sp. z.o.o, Poznan, Poland), transferred to the Petri dishes with a PMMA photoresist inside, and cultured for 24 h. Afterwards, the cells were fixed with 3.7% paraformaldehyde solution in PBS (phosphate buffered saline, pH 7.4, Sigma-Aldrich Sp. z.o.o, Poznan, Poland). After the fixation, the cells were washed with the PBS buffer dissolved in water, and finally washed out with deionized water. Such protocol

allows drying of the cells with no crystallization of salt on the sample surface. The contact microscope images of the T24 cell lines were acquired using 200 pulses of SXRs with exposure time of 20 s. Following exposure to the soft X-rays, the photoresist was cleaned using a 1% chlorox solution (sodium hypochlorite 5.25% w/w) to remove all residues of the sample. The photoresist was then developed in methyl isobutyl ketone and isopropyl alcohol (MIBK:IPA, 1:2 v/v) for 120 s. The development process results in a high resolution relief-map of the cellular structures within the photoresist, which was then viewed at high magnification by means of an atomic force microscope (AFM, NT-MDT Spectrum Instruments, Moscow, Russia).

The AFM scan was made in a semi-contact mode over an area of 80 × 80 μm^2 with 512 pixels per line and 25 × 25 μm^2 with 1024 pixels per line, respectively. The micrographs of the contact microscope images of the T24 cancer cells are shown in Figure 5a,b. In these images, the overall structures of the cells, including the central dense part (nucleus), are clearly visible.

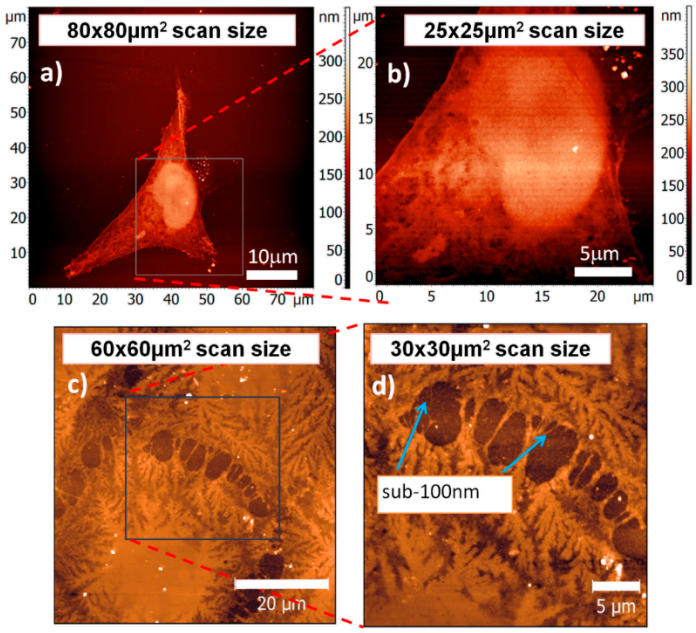

Figure 5. SXR contact microscopy images of fixed transitional cancer cell of the urine bladder (T24), FOV = 80 × 80 μm^2 and 25 × 25 μm^2 (**a**,**b**) and fixed epidermal cells (**c**,**d**) (Keratinocytes), FOV = 60 × 60 μm^2 and 30 × 30 μm^2. Images were obtained with SXR exposure of 200 pulses, 20 s and the photoresist was scanned using AFM microscope in semi-contact mode. Structures with sizes below 100 nm are visible.

Another sample used in the preliminary contact microscopy experiments was epidermal cell (Keratinocyte), as depicted in Figure 5c,d. The sample was prepared in collaboration with the Institute of Biotechnology, Warsaw University of Technology, Warsaw, Poland. The sample was cultured on PMMA photoresist in a controlled culture conditions. A Dulbecco's Modified Eagle's Culture Medium (DMEM, Sigma-Aldrich) supplemented with 1% L-glutamine, 1% penicillin/streptomycin, and 10% heat inactivated fetal bovine serum (Celbio, EuroClone S.p.A., Pero, MI, USA) was used as a culture medium. The culture medium was washed with PBS buffer solution followed by fixation and dehydration of the cells using paraformaldehyde 3.7% in phosphate buffered saline at 35 °C. The exposure of 200 SXR pulses, 20 s exposure time, was required to expose the PMMA photoresist and reach spatial resolution of approximately 80 nm half-pitch. The photoresist was treated with previously mentioned procedure and later scanned with AFM (AFM, NT-MDT Spectrum Instruments, Moscow, Russia) operating in semi-contact mode. Each image was 512 × 512 points over 60 × 60 μm^2 and

25×25 μm^2 in left and right images, respectively. As can be observed, structures with sizes below 100 nm are clearly visible. More details about this work can be found in [40,41].

4. Discussion and Conclusions

The SXR and EUV desktop microscopes, both full-field and contact-type, recently developed at the Institute of Optoelectronics, Military University of Technology, Warsaw, Poland, for imaging nanoscale objects were presented. All microscopes are based on laser plasma sources producing the EUV and SXR radiations through interaction of nanosecond laser pulses with double stream gas puff target. The imaging systems allow capturing magnified images of the samples, with 50–80 nm half-pitch spatial resolution and exposure time as low as few seconds. The microscopes are compact and allow obtaining images with a nanometer spatial resolution and short exposure time, which may open the possibility of their future commercialization. Those systems employing photons and not electrons, like in SEM, can obtain additional/complementary information about the sample under investigation. Moreover, those systems do not require coating with a conductive layer, such as in the SEM microscopes, to remove surface charges accumulated during the imaging. Although their spatial resolution cannot compete with electron based systems, it is much better that the visible light microscopes and comparable to synchrotron based microscopy systems and to Stimulated Emission Depletion microscopy (STED) [42,43]. Such table-top systems allow for a direct acquisition of a full field images, in contrary to STED acquisition operating in scanning mode, and do not require fluorescent bio markers or staining that modifies the morphology of the sample. Additionally, they use wavelengths that provide high optical contrast, either in biological (SXR microscope) or in all matter with thicknesses less than a few hundred nanometers (EUV microscope).

To distinguish between EUV/SXR full field microscopes and SXR contact microscope one has to notice, however, that although the contact microscopy lacks expensive optics and allows for high spatial resolution, limited in principle by the resolution of the underlying photoresist (for PMMA ~10 nm), the contact microscopy procedure causes the sample to be destroyed after imaging. It is because the resist, with the sample located on top, is being developed chemically after the exposure, which causes the sample to be irreversibly lost. In full-field microscopes the sample is located at some distance from the objective, without any contact with optics, detectors, etc., and can be later studied using other techniques (VIS, SEM, AFM microscopes, etc.), however, for the price of costly and still optically inefficient EUV and SXR optics. So, the choice of the technique is always related directly to the information that one wants to obtain from the samples investigated.

Acknowledgments: This work is supported by the National Science Centre, Opus program, grant agreement number UMO-2015/17/B/ST7/03718 and UMO-2015/19/B/ST3/00435, the National Centre for Research and Development, LIDER program; award # LIDER/004/410/L-4/12/NCBR/2013, the Education, Audiovisual and Culture Executive Agency (EACEA) Erasmus Mundus Joint Doctorate Program Project No. 2012-0033 and from the European Union's Horizon 2020 research and innovation program, under Laserlab-Europe IV, grant agreement No. 654148. The preparation of the biological cells has been supported by MEYS grant LG15013. We would like to thank to Andrzej Kowalik and Anna Rojek, from the Institute of Electronic Materials Technology (ITME), Warsaw, Poland for the preparation of the photoresist in their laboratory. We also acknowledge Tomasz Kobiela and Anna Sobiepanek, from the Faculty of Chemistry Warsaw University of Technology and Małgorzata Lekka, from the institute of Nuclear Physics Krakow, Poland for providing the biological samples used for contact microscopy experiments.

Author Contributions: Premyslaw Wachulak conceived and designed the experiments, performed the measurements, and wrote the paper; Alfio Torrisi performed the experiments and processed the data in EUV and SXR full field microscopy; Mesfin Ayele performed the contact microscopy experiments; Joanna Czwartos analyzed the samples in contact microscopy by the use of AFM; Andrzej Bartnik designed and developed gas puff target source; Lukasz Wegrzynski and Tomasz Fok helped in the development of the EUV microscope; Michal Odstrcil prepared neuron samples; Tomas Parkman, Sarka Salacova, and Jana Turnova, prepared other samples that were imaged, except for contact microscopy; Henryk Fiedorowicz conceived the gas puff target source and contact microscopy system.

Conflicts of Interest: The authors declare no conflict of interest. The founding sponsors had no role in the design of the study; in the collection, analyses, or interpretation of data; in the writing of the manuscript, or in the decision to publish the results.

References

1. Yelin, D.; Silberg, Y. Laser scanning third-harmonic generation microscopy in biology. *Opt. Express* **1999**, *5*, 169–175. [CrossRef] [PubMed]
2. Athanasiou, C.E.; Bellouard, Y. A monolithic microtensile tester for the investigation of silicon dioxide micromechanics, fabricated and operated by a femtosecond laser. *Micromachines* **2015**, *6*, 1365–1386. [CrossRef]
3. Technical Committee. ISO/TC20, Aircraft and space vehicles, Subcommittee SC14, Space systems and operations. In *Definitions of Solar Irradiance Spectral Categories*; ISO 21348; ISO: Geneva, Switzerland, 2007; pp. 6–7.
4. Le Gros, M.A.; McDermott, G.; Cinquin, B.P. Biological soft X-ray tomography on beamline 2.1 at the Advanced Light Source. *J. Synchrotron Radiat.* **2014**, *21*, 1–8. [CrossRef] [PubMed]
5. Chapman, H.N.; Barty, A.; Bogan, M.; Sebastien, B.; Frank, M.; Hau-Riege, S.; Marchesini, S.; Woods, B.; Sasa, B.; Benner, H.; et al. Femtosecond diffractive imaging with a soft-X-ray free-electron laser. *Nat. Phys.* **2006**, *2*, 839–843. [CrossRef]
6. Wilke, R.N.; Priebe, M.; Bartels, M.; Giewekemeyer, K.; Diaz, A.; Karvinen, P.; Salditt, T. Hard X-ray imaging of bacterial cells: Nano-diffraction and ptychographic reconstruction. *Opt. Express* **2012**, *20*, 19232–19254. [CrossRef] [PubMed]
7. Martz, D.H.; Selin, M.; von Hofsten, O.; Fogelqvist, E.; Holmberg, A.; Vogt, U.; Legall, H.; Blobel, G.; Seim, C.; Stiel, H.; et al. High average brightness water window source for short-exposure cryomicroscopy. *Opt. Lett.* **2012**, *37*, 4425–4427. [CrossRef] [PubMed]
8. Li, B.; Higashiguchi, T.; Otsuka, T.; Jiang, W.; Endo, A.; Dunne, P.; O'Sullivan, G. 'water window' sources: Selection based on the interplay of spectral properties and multilayer reflection bandwidth. *Appl. Phys. Lett.* **2013**, *102*, 1–5. [CrossRef]
9. Marino, S.; Palanco, S.; Gabás, M.; Romero, R.; Ramos-Barrado, J.R. Laser nano- and micro-structuring of silicon using a laser-induced plasma for beam conditioning. *Nanotechnology* **2015**, *26*, 55303. [CrossRef] [PubMed]
10. Van Malderen, S.J.M.; van Elteren, J.T.; Vanhaecke, F. Submicrometer imaging by laser ablation–Inductively coupled plasma mass spectrometry via signal and image deconvolution approaches. *Anal. Chem.* **2015**, *87*, 6125–6132. [CrossRef] [PubMed]
11. Schneider, G. Cryo X-ray microscopy with high spatial resolution in amplitude and phase contrast. *Ultramicroscopy* **1998**, *75*, 85–104. [CrossRef]
12. Chao, W.; Fischer, P.; Tyliszczak, T.; Rekawa, S.; Anderson, E.; Naulleau, P. Real space soft X-ray imaging at 10 nm spatial resolution. *Opt. Express* **2012**, *20*, 9777–9783. [CrossRef] [PubMed]
13. Simons, H.; King, A.; Ludwig, W.; Detlefs, C.; Pantleon, W.; Schmidt, S.; Snigireva, I.; Snigirev, A.; Poulsen, H.F. Dark-field X-ray microscopy for multiscale structural characterization. *Nat. Commun.* **2015**, *6*, 6098. [CrossRef] [PubMed]
14. Andrews, J.C.; Meirer, F.; Liu, Y.; Mester, Z.; Pianetta, P. Transmission X-ray microscopy for full-field nano imaging of biomaterials. *Microsc. Res. Tech.* **2011**, *74*, 671–681. [CrossRef] [PubMed]
15. Kim, K.W.; Kwon, Y.; Nam, K.; Lim, J.; Kim, K.W.; Chon, K.; Kim, B.; Kim, D.E.; Kim, J.; Ahn, B.N.; et al. Compact soft X-ray transmission microscopy with sub-50 nm spatial resolution. *Phys. Med. Biol.* **2006**, *51*, N99–N107. [CrossRef] [PubMed]
16. Kim, H.T.; Kim, I.J.; Kim, C.M.; Yu, T.J.; Lee, S.K.; Sung, J.H.; Yoon, J.W.; Yun, H.; Jeong, T.M.; Choi, I.W.; et al. Single-shot nanometer-scale Fourier transform hologram using Ni-like Ag X-ray laser. In *Springer Proceedings in Physics*; Springer: New York, NY, USA, 2010; pp. 323–328.
17. Park, J.J.J.; Kim, D.S.; Jeon, S.C.; Park, J.J.J.; Lee, K.H.; Lee, J.; Kim, K.N.; Yoo, J.J.; Nam, C.H. Table-top soft X-ray microscope adopting a PMMA phase-reversal zone plate. *Opt. Lett.* **2009**, *2*, 5–6.
18. Dierolf, M.; Thibault, P.; Menzel, A.; Kewish, C.M.; Jefimovs, K.; Schlichting, U.; Von König, K.; Bunk, O.; Pfeiffer, F. Ptychographic coherent diffractive imaging of weakly scattering specimens. *New J. Phys.* **2010**, *12*, 35017. [CrossRef]
19. Marconi, M.C.; Wachulak, P.W. Extreme ultraviolet lithography with table top lasers. *Prog. Quantum Electron.* **2010**, *34*, 173–190. [CrossRef]

20. Wachulak, P.W.; Wegrzynski, L.; Bartnik, A.; Fok, T.; Jarocki, R.; Kostecki, J.; Szczurek, M.; Fiedorowicz, H. Characterization of a dual-gas multi-jet gas puff target for high-order harmonic generation using extreme ultraviolet shadowgraphy. *Laser Part. Beams* **2013**, *31*, 219–227. [CrossRef]
21. Brewer, C.A.; Brizuela, F.; Wachulak, P.; Martz, D.H.; Chao, W.; Anderson, E.H.; Attwood, D.T.; Vinogradov, A.V.; Artyukov, I.A.; Ponomareko, A.G.; et al. Single-shot extreme ultraviolet laser imaging of nanostructures with wavelength resolution. *Opt. Lett.* **2008**, *33*, 518–520. [CrossRef] [PubMed]
22. Wachulak, P.W.; Brewer, C.A.; Brizuela, F.; Menoni, C.S.; Chao, W.; Anderson, E.H.; Bartels, R.A.; Rocca, J.J.; Marconi, M.C. Analysis of extreme ultraviolet microscopy images of patterned nanostructures based on a correlation method. *J. Opt. Soc. Am.* **2008**, *25*, B20–B26. [CrossRef]
23. Wachulak, P.W.; Marconi, M.C.; Bartels, R.A.; Menoni, C.S.; Rocca, J.J. Soft X-ray laser holography with wavelength resolution. *J. Opt. Soc. Am.* **2008**, *25*, 1811–1814. [CrossRef]
24. Vaschenko, G.; Brizuela, F.; Brewer, C.; Grisham, M.; Mancini, H.; Menoni, C.S.; Marconi, M.C.; Rocca, J.J.; Chao, W.; Liddle, J.; et al. Nanoimaging with a compact extreme-ultraviolet laser. *Opt. Lett.* **2005**, *30*, 2095–2097. [CrossRef] [PubMed]
25. Juschkin, L.; Freiberger, R.; Bergmann, K. EUV microscopy for defect inspection by dark-field mapping and zone plate zooming. *J. Phys. Conf. Ser.* **2009**, *186*, 12030. [CrossRef]
26. Legall, H.; Blobel, G.; Stiel, H.; Sandner, W.; Seim, C.; Takman, P.; Martz, D.H.; Selin, M.; Vogt, U.; Hertz, H.M.; et al. Compact X-ray microscope for the water window based on a high brightness laser plasma source. *Opt. Express* **2012**, *20*, 18362–18369. [CrossRef] [PubMed]
27. Kirz, J.; Jacobsen, C.; Howells, M. Soft X-ray microscopes and their biological applications. *Q. Rev. Biophys.* **1995**, *28*, 33–130. [CrossRef] [PubMed]
28. Cheng, P.C.; Feder, R.; Shinozaki, D.M.; Tan, K.H.; Eason, R.W.; Michette, A.; Rosser, R.J. Soft X-ray contact microscopy. *Nucl. Instrum. Methods Phys. Res. A* **1986**, *246*, 668–674. [CrossRef]
29. Ford, T.W.; Stead, A.D.; Cotton, R.A. Soft X-ray contact microscopy of biological materials. *Electron Microsc. Rev.* **1991**, *4*, 269–292. [CrossRef]
30. Kado, M.; Kishimoto, M.; Tamotsu, S.; Yasuda, K.; Aoyama, M.; Shinohara, K. Imaging of fine structures of cellular organelles in hydrated biological cells by a soft X-ray microscope combined with a fluorescence microscope. In Proceedings of the Conference of X-ray Lasers and Coherent X-ray Sources: Development and Applications X, San Diego, CA, USA, 25 August 2013.
31. Fiedorowicz, H.; Bartnik, A.; Jarocki, R.; Kostecki, J.; Krzywinski, J.; Mikołajczyk, J.; Rakowski, R.; Szczurek, A.; Szczurek, M. Compact laser plasma EUV source based on a gas puff target for metrology applications. *J. Alloys Compd.* **2005**, *401*, 99–103. [CrossRef]
32. Ul Ahad, I.; Bartnik, A.; Fiedorowicz, H.; Kostecki, J.; Korczyc, B.; Ciach, T.; Brabazon, D. Surface modification of polymers for biocompatibility via exposure to extreme ultraviolet radiation. *J. Biomed. Mater. Res. A* **2014**, *102*, 3298–3310. [CrossRef] [PubMed]
33. Adjei, D.; Wiechec, A.; Wachulak, P.; Ayele, M.; Lekki, J.; Kwiatek, W.; Bartnik, A.; Davídková, M.; Vyšín, L.; Juha, L.; et al. DNA strand breaks induced by soft X-ray pulses from a compact laser plasma source. *Radiat. Phys. Chem.* **2016**, *120*, 17–25. [CrossRef]
34. Wachulak, P.; Bartnik, A.; Skorupka, M.; Kostecki, J.; Jarocki, R.; Szczurek, M.; Wegrzynski, L.; Fok, T.; Fiedorowicz, H. Water-window microscopy using a compact, laser-plasma SXR source based on a double-stream gas-puff target. *Appl. Phys. B Lasers Opt.* **2013**, *111*, 239–247. [CrossRef]
35. Heck, J.; Attwood, D.; Berkeley, E.; Meyer-ilse, W.; Anderson, E. Resolution determination in X-ray microscopy: An analysis of the effects of partial coherence and illumination spectrum. *J. X-ray Sci. Technol.* **1998**, *8*, 95–104. [PubMed]
36. Wachulak, P.; Torrisi, A.; Nawaz, M.; Bartnik, A.; Adjei, D.; Vondrová, Š.; Turňová, J.; Jančarek, A.; Limpouch, J.; Vrbová, M.; et al. A Compact "water window" microscope with 60 nm spatial resolution for applications in biology and nanotechnology. *Microsc. Microanal.* **2015**, *21*, 1214–1223. [CrossRef] [PubMed]
37. Wachulak, P.; Torrisi, A.; Bartnik, A.; Adjei, D.; Kostecki, J.; Wegrzynski, L.; Jarocki, R.; Szczurek, M.; Fiedorowicz, H. Desktop water window microscope using a double-stream gas puff target source. *Appl. Phys. B* **2015**, *118*, 573–578. [CrossRef]
38. Wachulak, P.; Torrisi, A.; Bartnik, A.; Węgrzyński, Ł.; Fok, T.; Fiedorowicz, H. A desktop extreme ultraviolet microscope based on a compact laser-plasma light source. *Appl. Phys. B* **2016**, *123*, 1–5. [CrossRef]

39. Torrisi, A.; Wachulak, P.; Węgrzyński, Ł.; Fok, T.; Bartnik, A.; Parkman, T.; Vondrová, Š.; Turňová, J.; Jankiewicz, B. J.; Bartosewicz, B.; et al. A stand-alone compact EUV microscope based on gas-puff target source. *J. Microsc.* **2017**, *265*, 251–260. [CrossRef] [PubMed]
40. Ayele, M.; Czwartos, J.; Adjei, D.; Wachulak, P.; Ahad, I.U.; Bartnik, A.; Wegrzynski, Ł.; Szczurek, M.; Jarocki, R.; Fiedorowicz, H.; et al. Contact microscopy using a compact laser produced plasma soft X-ray source. *Acta Phys. Pol. A* **2016**, *129*, 237–240. [CrossRef]
41. Ayele, M.; Wachulak, P.; Czwartos, J.; Adjei, D.; Bartnik, A.; Wegrzynski, Ł.; Szczurek, M.; Pina, L.; Fiedorowicz, H. Development and characterization of a laser-plasma soft X-ray source for contact microscopy. *Nucl. Instr. Meth. B* **2017**, in press.
42. Otomo, K.; Hibi, T.; Kozawa, Y. STED microscopy—Super-resolution bio-imaging utilizing a stimulated emission depletion. *Microscopy* **2015**, *64*, 1–10. [CrossRef] [PubMed]
43. Farahani, J.; Schibler, M.; Bentolila, L. Stimulated emission depletion (STED) microscopy: From theory to practice. *Microsc. Sci. Technol. Appl. Educ.* **2010**, *2*, 1539–1547.